

AROD-8045.10-RC

AD 745909

Kinetics and Mechanisms of Synergetic
Pressure-Sintering and Mechanical Behavior
of High-Strength Ceramics

Final Report

to

U.S. Army Research Office-Durham

Grant No. DA-AROD-D-31-124-G1106

for the period

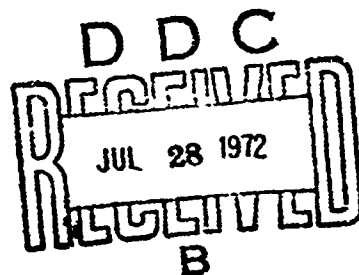
1 April, 1969 to 30 April, 1972

by

R. M. Spriggs
D. P. H. Hasselman
M. R. Notis
R. B. Runk
C. J. P. Steiner
D. A. Krohn
R. H. Smoak

Reproduced by
NATIONAL TECHNICAL
INFORMATION SERVICE
U.S. Department of Commerce
Springfield VA 22151

Approved for public release; distribution
unlimited. The findings in this report are
not to be construed as an official Depart-
ment of the Army position, unless so desig-
nated by other authorized documents.



May 30, 1972

Physical Ceramics Laboratory
Materials Research Center
Lehigh University
Bethlehem, Pa. 18015

5

Unclassified
Security Classification

DOCUMENT CONTROL DATA - R & D

(Security classification of title, body of abstract and indexing annotations must be entered when the overall report is classified)

1. ORIGINATING ACTIVITY (Corporate author)		2a. REPORT SECURITY CLASSIFICATION Unclassified	
Lehigh University		2b. GROUP NA	
3. REPORT TITLE Kinetics and Mechanisms of Synergetic Pressure-Sintering and Mechanical Behavior of High-Strength Ceramics			
4. DESCRIPTIVE NOTES (Type of report and inclusive dates) Final Report: 1 April 1969 - 30 April 1972			
5. AUTHOR(S) (First name, middle initial, last name)		6. REPORT DATE 30 May 1972	
R. M. Spriggs D. P. H. Hasselman M. R. Notis		7a. TOTAL NO. OF PAGES 52	
		7b. NO. OF REFS NA	
8. CONTRACT OR GRANT NO. DA-ARO-D-31-124-G1106		9a. ORIGINATOR'S REPORT NUMBER(S) NA	
b. PROJECT NO. 20061102B32D		9b. OTHER REPORT NO(S) (Any other numbers that may be assigned this report) 8045.10-MC	
10. DISTRIBUTION STATEMENT Approved for public release; distribution unlimited.			
11. SUPPLEMENTARY NOTES None		12. SPONSORING MILITARY ACTIVITY U. S. Army Research Office-Durham Box CM, Duke Station Durham, North Carolina 27706	
13. ABSTRACT <p>This report presents a summary of the following research efforts: (1) a major effort was devoted to studying the synergetic effect of the γ to α alumina phase transformation on pressure-sintering kinetics of high-density alumina ceramics. (2) An extensive program was also initiated with the purpose of relating diffusion coefficients observed for ceramics subjected to pressure-sintering or press-forging operations with interdiffusion coefficients observed in diffusion experiments. (3) In addition to the studies on basic mechanisms in the densification kinetics of ceramics, considerable attention was also devoted to studies of the mechanical behavior of ceramic materials. (4) Additional studies of the mechanical behavior of ceramic materials involved an analysis of fracture energies.</p>			
14. KEY WORDS Synergetic Pressure-Sintering High-Strength Ceramics Ceramics Magnesium Aluminate Spinel			

DD FORM 1 NOV 68 1473 REPLACES DD FORM 1473, 1 JAN 64, WHICH IS
OBsolete FOR ARMY USE.

I

Unclassified
Security Classification

Kinetics and Mechanisms of Synergetic
Pressure-Sintering and Mechanical Behavior
of High-Strength Ceramics

Final Report
to
U.S. Army Research Office-Durham
Grant No. DA-AROD-D-31-124-G1106
for the period
1 April, 1969 to 30 April, 1972

by

R. M. Spriggs
D. P. H. Hasselman
M. R. Notis
R. B. Runk
C. J. P. Steiner
D. A. Krohn
R. H. Smoak

May 30, 1972

Physical Ceramics Laboratory
Materials Research Center
Lehigh University
Bethlehem, Pa. 18015

IV

FINAL REPORT

1. ARO-D PROPOSAL NUMBER 8045-MC
2. PERIOD COVERED BY REPORT: 1 April 1969 to 30 April 1972
3. TITLE OF PROPOSAL: Kinetics and Mechanisms of Synergetic Press-Forging of High-Strength, Transparent Ceramics"
4. CONTRACT OR GRANT NUMBER: DA-ARO-D-31-124-G1106
5. NAME OF INSTITUTION: Lehigh University, Bethlehem, Pa.
6. AUTHOR(S) OF REPORT: R. M. Spriggs, D. P. H. Hasselman, M. R. Notis, D. A. Krohn, C. J.-P. Steiner and R. H. Smoak
7. LIST OF MANUSCRIPTS SUBMITTED OR PUBLISHED UNDER ARO-D SPONSORSHIP DURING THIS PERIOD, INCLUDING JOURNAL REFERENCES:
 - a. "The Kinetics of the Gamma-to Alpha Alumina Phase Transformation", J. Amer. Ceram. Soc., 54, 412-13 (1971).
 - b. "Relation of Flaw Size to Mirror in the Fracture of Glass", J. Amer. Ceram. Soc., 54, 411 (1971).
 - c. "Synergetic Pressure-Sintering of Al_2O_3 ", J. Amer. Ceram. Soc., 55, 115-16 (1972).
 - d. "Thermal-Stress Fracture of a Thermomechanically Strengthened Aluminosilicate Ceramic", J. Amer. Ceram. Soc., 55, 198-201 (1972).
 - e. "Static and Cyclic Fatigue Behavior of a Polycrystalline Alumina", J. Amer. Ceram. Soc., 55, 208-11 (1972).
 - f. "Surface Fracture Energy and the Work of Fracture of Brittle Solids". Submitted to Philosophical Magazine.
 - g. "The Griffith Approach to Brittle Fracture and Plastic Flow in Glass" submitted to American Ceramic Society.
8. SCIENTIFIC PERSONNEL SUPPORTED BY THIS PROJECT AND DEGREES AWARDED THIS REPORTING PERIOD:

R. M. Spriggs, Principal Investigator (Vice-President of Administration Professor, Metallurgy and Materials Science)

R. B. Runk, Co-Investigator
(Associate Professor, Metallurgy and Materials Science, now with Western Electric, Princeton, N. J.)

D. P. H. Hasselman, Co-Investigator
(Associate Professor, Metallurgy and Materials Science, Director Physical Ceramics Laboratory, Materials Research Center)

3. (Cont'd)

M. R. Notis, Co-Investigator
(Assistant Professor, Metallurgy and Materials Science)

C. J.-P. Steiner, Research Assistant
Ph.D. Degree: "The Gamma to Alpha Alumina Phase Transformation and Synergetic Pressure-Sintering of High Density Polycrystalline Alumina."

D. A. Krohn, Research Assistant
(Ph.D. Candidate, Metallurgy and Materials Science)

R. H. Smoak, Research Assistant
(Ph.D. Candidate, Metallurgy and Materials Science)

PROGRAM SUMMARY

In this program a major effort was devoted to studying the synergetic effect of the γ to α alumina phase transformation on pressure-sintering kinetics of high-density alumina ceramics. An X-ray study of the kinetics of the γ to α alumina phase transformation indicated that a synergetic effect of the phase transformation would be most advantageous at higher heating rates in the pressure-sintering operation which was verified subsequently by experiment. This study resulted in two separate publications in the Journal of the American Ceramic Society of which 25 reprints were submitted to ARO-D previously.

An extensive program was also initiated with the purpose of relating diffusion coefficients observed for ceramics subjected to pressure-sintering or press-forging operations with interdiffusion coefficients observed in diffusion experiments. A magnesium aluminate spinel was chosen as model material. Background, scope and progress made to date is reported in Appendix I, which represents the Ph.D. thesis proposal of Mr. R. H. Smoak. This study is being continued with funding from other sources.

In addition to the studies on basic mechanisms in the densification kinetics of ceramics, considerable attention was also devoted to studies

8. (Cont'd)

M. R. Notis, Co-Investigator
(Assistant Professor, Metallurgy and Materials Science)

C. J.-P. Steiner, Research Assistant
Ph.D. Degree: "The Gamma to Alpha Alumina Phase Transformation and Synergetic Pressure-Sintering of High Density Polycrystalline Alumina."

D. A. Krohn, Research Assistant
(Ph.D. Candidate, Metallurgy and Materials Science)

R. H. Smoak, Research Assistant
(Ph.D. Candidate, Metallurgy and Materials Science)

PROGRAM SUMMARY

In this program a major effort was devoted to studying the synergetic effect of the γ to α alumina phase transformation on pressure-sintering kinetics of high-density alumina ceramics. An X-ray study of the kinetics of the γ to α alumina phase transformation indicated that a synergetic effect of the phase transformation would be most advantageous at higher heating rates in the pressure-sintering operation which was verified subsequently by experiment. This study resulted in two separate publications in the Journal of the American Ceramic Society of which 25 reprints were submitted to ARO-D previously.

An extensive program was also initiated with the purpose of relating diffusion coefficients observed for ceramics subjected to pressure-sintering or press-forging operations with interdiffusion coefficients observed in diffusion experiments. A magnesium aluminate spinel was chosen as model material. Background, scope and progress made to date is reported in Appendix I, which represents the Ph.D. thesis proposal of Mr. R. H. Smoak. This study is being continued with funding from other sources.

In addition to the studies on basic mechanisms in the densification kinetics of ceramics, considerable attention was also devoted to studies

of the mechanical behavior of ceramic materials. The static and cyclic fatigue behavior of a polycrystalline alumina was studied, which showed the presence of a strong cyclic fatigue mechanism in addition to the well-known static fatigue mechanism. Also, the fracture of glass was analyzed which showed a direct relation between flaw size and mirror radius of the fracture surface. In addition, the thermal stress fracture characteristics of ceramics strengthened by surface compression was investigated experimentally as well as theoretically. The study clearly showed the advantage of surface compression strengthening to circumvent the severe problem of the generally low thermal stress resistance of ceramics. These three studies on mechanical behavior all resulted in a publication in the Journal of the American Ceramic Society of which 25 reprints were forwarded to ARO-D previously.

Additional studies of the mechanical behavior of ceramic materials involved an analysis of fracture energies. In a paper submitted to the Philosophical Magazine (reproduced in Appendix II) it was suggested that measured values of fracture energy in part consist of unrecoverable elastic energy, such that discrepancies between surface free energy and fracture energy do not have to be attributed to energy dissipative processes such as plastic flow.*

Finally the fracture behavior of glass was analyzed in terms of dislocation mechanisms which resulted in a paper submitted for publication to the American Ceramic Society (reproduced in Appendix III).*

* (Note: Since Appendices II and III have also been submitted in manuscript form to AROD, They (along with App.I) are reproduced in their entirety in only 25 copies of this final report.)

Appendix I

PRESSURE SINTERING KINETICS AND DIFFUSION IN POLYCRYSTALLINE MAGNESIUM ALUMINATE SPINEL

The fabrication of ceramic bodies by pressure sintering makes it possible to obtain high density, fine grained materials with marked improvements in mechanical properties at a temperature significantly lower than the temperature required for a conventional sintering process. Since density and microstructure have a large influence upon the mechanical behavior of ceramic bodies a knowledge of means to control these factors becomes extremely important. In order to improve the pressure sintering process it is necessary that a better understanding of the basic mechanisms of densification be developed.

Densification Models

The model on which most analyses of diffusion-controlled densification phenomena are based is that of Nabarro (1) and Herring (2). A diffusional mechanism is assumed with vacancy migration occurring from regions under tensile stresses (vacancy sources) to those subject to compressive stresses (vacancy sinks). The pressure-temperature regime where this model is valid will yield a linear relationship between $\log \dot{\epsilon}$ and $\log \sigma_e$ with a slope of unity.* This model, originally derived to explain steady-state creep behavior, has been modified to account for the rate of densification during the final stages of pressure sintering.

* $\dot{\epsilon}$ is the strain rate and σ_e is the effective stress on the specimen.

Direct evidence that the Nabarro-Herring mechanism of stress-directed vacancy flow is operative during creep was obtained by Tien and Gamble (3) in their studies on the influence of applied stress and stress sense on grain boundary precipitate morphology during creep. Before creep studies were carried out the microstructure of their test specimens* was examined and found to consist of a regular array of grains on the order of $20 \sim 50 \mu\text{m}$ in size and containing a uniform distribution of coherent precipitates. After both tensile and compressive creep to a point of 5% strain it was found that the boundaries in tension were denuded of precipitates while the volume fraction of precipitates at boundaries in compression was increased. By use of the electron microprobe to analyze the chemistry of the grain boundary areas it was found that the denuded boundaries were rich in chromium while the chromium content of the boundaries containing high percentages of precipitates was depleted. Since chromium is known to stabilize the matrix at the expense of the precipitates it was concluded (3) that the Cr diffused by way of stress-directed diffusional flow during creep in the manner described by Nabarro (1).

The final stage pressure sintering models as derived from Nabarro-Herring creep theory contain a density function, $f(D)$, to account for the difference between the effective stress and the applied stress on the specimen. The generalized equation for the final stage of pressure sintering is $\dot{\epsilon} = K \sigma_e^n$. (Here σ_e , the effective stress on the specimen,

* A nickel based superalloy of composition (wt. percent) Ni - 16Cr - 5Al - 4Ta.

is equal to $\sigma_a f(D)$ where σ_a is the applied stress; K is a constant.) The strain rate during pressure sintering can be equated to the densification rate through the relation $\dot{\epsilon}_{p.s.} = \frac{-1}{t} \frac{d\ell}{dt} = \frac{1}{\rho} \frac{dp}{dt}$ where $\dot{\epsilon}$ and t are the instantaneous relative density of the compact and the compact length, respectively (4).

In order to determine a value for the constant K (which includes the diffusion coefficient) from experimental data, it is necessary to have an expression for $f(D)$. Various investigators (4-7) have proposed such expressions and demonstrated their applicability with original data. However these expressions (given in Table I) have been analyzed by Coble (8) and found to yield the same result within a factor of four. The values of the functions converge to one as the relative density approaches unity so that at high density the choice of a density function should not materially affect the value of the effective stress.

Coble (9) has also derived a pressure sintering model for the case where diffusion via grain boundaries plays the major role in the densification process. This model, along with the model based on lattice diffusion, is given in Table II.

Some studies of creep of ceramic materials have been successfully modeled by the Nabarro-Herring theory. Coble (9) has noted that work on polycrystalline Al_2O_3 by Folweiler (10), by Warshaw (11) and by Beauchamp, et al. (12) indicates that it exhibits typical Nabarro-Herring creep behavior. This was also true for BeO as studied by Chang (13) and by Chandler, et al. (14). The diffusion coefficients calculated from the Nabarro-Herring model

TABLE I

Equations to Relate Applied Stress to Effective Stress

$$(\sigma_{\text{eff}} = \sigma_a f(D))$$

<u>Investigator</u>	<u>f(D)</u>
McClelland (5)	$1/(1-P^{2/3})$
Spriggs and Vasilos (6)	$1+2P$
Rossi (4)	$1+bP$
Farnsworth and Coble (7)	$\frac{1}{P}$

b = constant, P = relative porosity ($P = 1-\rho$)

TABLE II

Pressure Sintering Models Based on the Nabarro-Herring Creep Mechanism

For a lattice diffusion controlled process (8) :

$$\dot{\epsilon}_{p.s.} = \frac{40D_L\Omega}{3d^2kT} \left(\frac{\sigma_a}{\rho} + \frac{2\gamma}{r} \right)$$

For a grain boundary diffusion controlled process (8) :

$$\dot{\epsilon}_{p.s.} = \frac{47.5D_b w\Omega}{d^3kT} \left(\frac{\sigma_a}{\rho} + \frac{2\gamma}{r} \right)$$

- $\dot{\epsilon}_{p.s.}$ = steady-state strain rate during pressure sintering,
- D_L = lattice diffusion coefficient,
- Ω = vacancy volume,
- d = grain size (diameter),
- σ_a = applied stress,
- γ = surface energy of the pore,
- r = pore radius,
- ρ = relative density of the compact,
- D_b = grain boundary diffusion coefficient,
- w = effective grain boundary width,
- k = Boltzman's constant, and
- T = temperature in degrees kelvin.

were the same as the values obtained from diffusion measurements within the estimated error limits for their experiments.

However, there is a great body of data in the literature in which the diffusion coefficient calculated by the Nabarro-Herring model is several orders of magnitude larger than the intrinsic diffusion coefficients. Some of this information is shown in Figures 1 and 2 which were taken from an article by Vasilos and Spriggs (15).

These discrepancies in diffusion coefficients are only one of the factors which have led investigators to attempt a more comprehensive explanation of densification phenomena. A serious fault of the Nabarro-Herring creep theory is that it implies that grain elongation will occur during deformation when in fact this is almost never observed to occur. The model also assumes the relaxation of shear stresses at the grain boundary by a viscous relaxation phenomenon but the contribution of this relaxation mechanism is assumed to be unimportant in the deformation process. Creep studies at low stress levels have also revealed that scratch off-setting, grain rotation, and granular surface roughening while an equiaxed grain structure is maintained can occur (16). These observations are consistent with the description of creep as a grain boundary sliding process.

The fact that a grain boundary sliding process can contribute to the creep of metals was reported as early as 1913 (17). However it was not until the early sixties that investigators realized that when creep occurs by a diffusional mechanism grain boundary sliding must occur to maintain specimen coherency (18). Creep deformation may also be regarded as due to grain

Figure 1.
from (15).

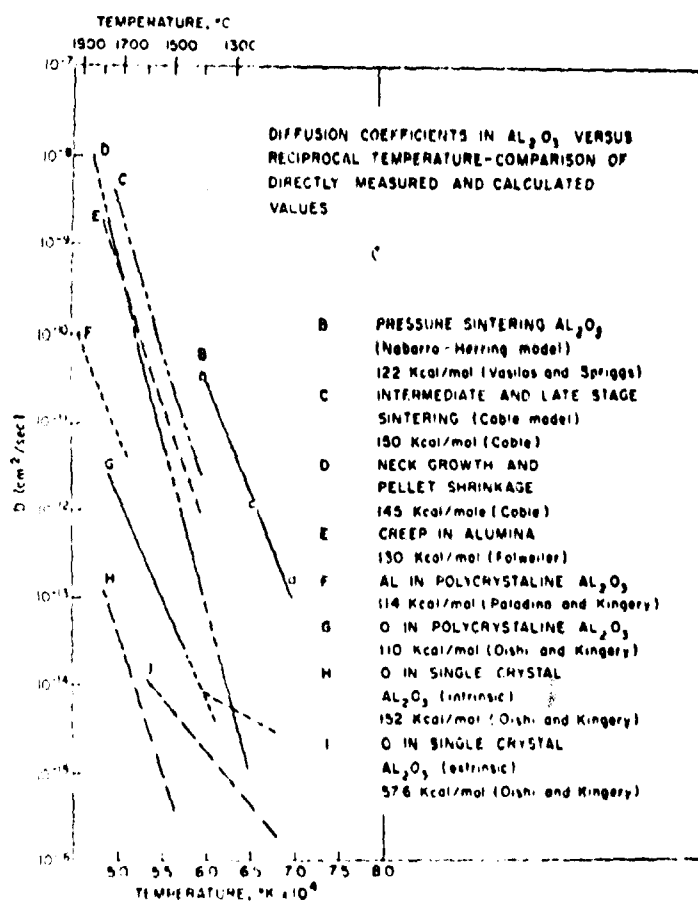
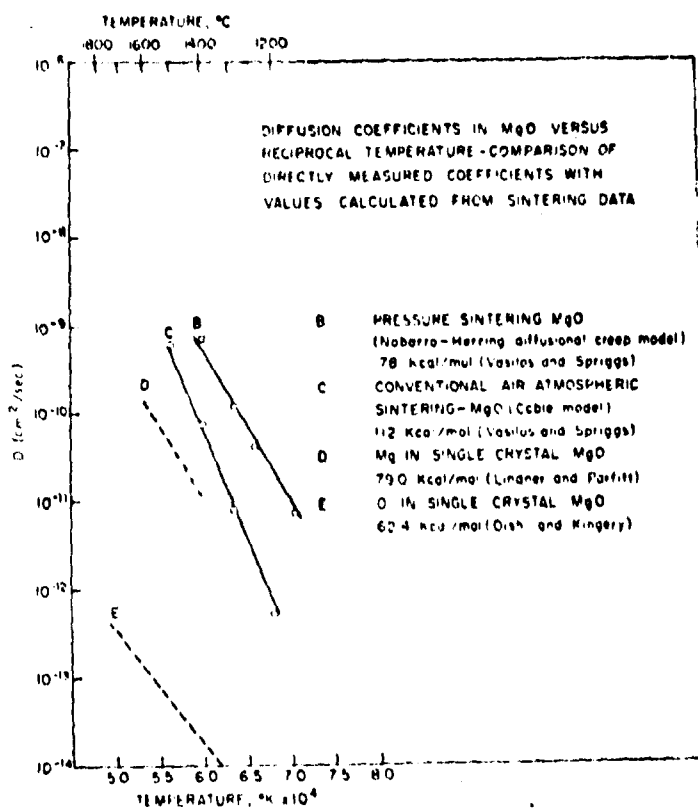


Figure 2.
from (15).



boundary sliding with diffusion of ions to accomodate incompatabilities which appear at the grain surfaces (19). Whichever approach to grain boundary sliding is taken the two concepts are physically identical and when correctly modeled they yield precisely the same result for the creep rate (20).

The grain boundary sliding processes responsible for creep of polycrystalline solids can be thought of in the following way. Due to the resolved shear stresses acting on the grain boundaries, adjacent grains may undergo a translation with respect to one another. However this translation (or grain boundary sliding) generates incompatabilities where the boundary deviates from a perfect plane. In order for sliding to continue it is necessary that an accomodation process occur. Generally it is the accomodation of these incompatabilities which controls the extent and rate of sliding (19). The accomodation may be purely elastic. Elastic stresses build up at points of boundary curvature until they balance the applied ones. At high temperatures ($T \geq 0.5 T_M$) other accomodation processes are possible. High temperatures combined with low applied stresses are conditions under which the stresses built up at a non-planar boundary may be relaxed by a diffusive flux of vacancies from areas of the boundary in tension to those areas in compression. And for conditions of high temperatures and high applied stress levels the accomodation process may occur by plastic flow due to dislocation motion.

Gifkins and Snowden (21) have examined the problem of including grain boundary sliding contributions to creep of metals and metal alloys. Based on the idea of the movement of double ledges or protrusions along

the grain boundary these investigators have derived an equation to predict the rate of sliding of a boundary oriented at 45° to the applied stress. However this equation, given in Table III, gave sliding rates approximately 30 times larger than observed experimentally when applied to the sliding rates of lead bicrystals.

The most comprehensive analysis of creep due to grain boundary sliding accommodated at triple points and grain boundary ledges has been presented by Raj and Ashby (19). These investigators discuss the process of sliding with diffusional accommodation and derive a general equation for the sliding rate of nonplanar boundaries. This equation, given in Table III, is based on the case where sliding occurs at a boundary containing rectangular steps and where these steps can be described in terms of their height, width, and spacing by a Fourier series (19).

As an approximation of the microstructure of a polycrystalline solid, a two-dimensional, hexagonal array of grains can be used. The grain boundary shape of this hexagonal array can then be approximated by a sine wave of amplitude, $d/2$ and wavelength, $2d$ where d is the grain size as shown in Figure 3. By use of these simplifying assumptions the equation developed by Raj and Ashby (19) (given in Table III) can be used to obtain an expression for the engineering-shear strain rate as shown in equation 1.

$$\dot{\gamma} = \frac{2U}{d} = \frac{40 \tau_a \Omega D_\ell}{d^2 kT} \left[1 + \frac{\pi \delta D_b}{\lambda D_\ell} \right] \quad (1)$$

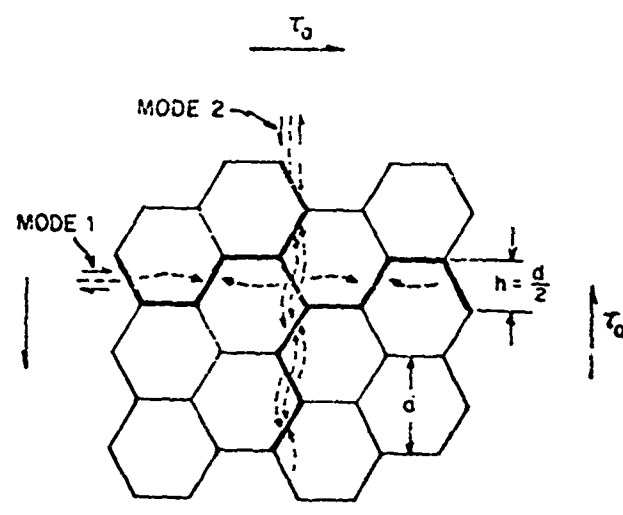


Fig. 3. -A polycrystal, idealized as an array of hexagons can deform by sliding in two orthogonal modes. Broken lines show the vacancy flux (19).

TABLE III

Model developed by Gifkins and Snowden (21):

$$\dot{S} = \frac{\alpha \sigma D_b \Omega}{L k T}$$

Model developed by Raj and Ashby (19):

$$\dot{\frac{S}{U}} = \frac{2 \tau_a \Omega \lambda D_l}{\pi k T h^2} \left[\sum_{n=1}^{\infty} \left\{ \frac{\left(\frac{2}{n\pi} \sin \frac{n\pi w}{\lambda} \right)^2}{\frac{1}{n} + \frac{\pi \delta D_b}{\lambda D_l}} \right\} \right]$$

$\dot{\frac{S}{U}}$ = grain boundary sliding rate

α = constant approximately equal to 2

σ = applied stress

D_b = grain boundary diffusion coefficient

Ω = vacancy volume

L = length of the grain boundary protrusion

τ_a = applied shear stress

λ = the periodicity or "wavelength" of the boundary

D_l = lattice diffusion coefficient

h = total height of the boundary protrusion

w = width of the grain boundary protrusion

δ = grain boundary width

k, T = have their usual meanings

Note that if the second term within the brackets is $\ll 1$ this equation reduces to an expression similar to one obtained from the Nabarro-Herring stress-directed diffusional model (1,2). Alternatively, if the second term within the brackets is $\gg 1$ this equation yields results similar to those obtained by Coble (9) for grain boundary diffusion controlled creep.

Up until the present time it has not been possible to obtain conclusive evidence as to the role which diffusion plays in the creep deformation of ceramic bodies. One of the major reasons for this is the lack of good diffusion data taken on polycrystalline specimens. The use of an intrinsic diffusion coefficient obtained on a single crystal of high purity by tracer diffusion techniques is not an appropriate value for a test of a densification model. The factors known to influence the diffusion coefficient in polycrystalline bodies such as the presence of grain boundaries, impurity content and distribution, and the dislocation density are not taken into account in making such a comparison.

In order to further our understanding of densification phenomena, there is a need for a set of unequivocal diffusion and densification experiments designed to yield diffusion coefficients under experimental conditions as nearly identical as possible. With such data at hand it should then be possible to explain the observed discrepancies between predicted behavior and that actually observed during the densification process. To obtain such information a program involving a multicomponent oxide, magnesium aluminate spinel, is outlined in the following section.

Purpose of Investigation

The purpose of the proposed investigation is four-fold: (1) to study the densification kinetics of a multicomponent oxide; (2) to obtain an appropriate model for the densification process and from the model to obtain diffusion coefficients and an activation energy for diffusion; (3) to perform diffusion experiments on the polycrystalline specimens formed during the pressure sintering experiments so that diffusion coefficients can be obtained on specimens whose structure and chemical makeup are as similar as possible to that of the pressure sintered specimens; and (4) to explain in terms of basic mechanisms the observed densification behavior of the multicomponent compound.

Method of Investigation

The compositions to be used in this investigation will be selected in the spinel solid solution region within the $MgO-Al_2O_3$ phase diagram. Several features of this system make it attractive for study. The compound $MgAl_2O_4$ is regarded as a model material and is representative of other spinel-type compounds such as $MgCr_2O_4$, $NiAl_2O_4$, $NiCr_2O_4$, etc. Detailed studies of the crystal chemistry of $MgAl_2O_4$ have been made and the locations of various cations in the spinel lattice have been determined (22,23). Spinel is of importance in itself due to its applications as a transparent armor candidate, as a high strength-low porosity substrate for epitaxially deposited silicon integrated circuits, and as a bonding phase in high alumina refractories.

A. Pressure Sintering Experiments

Spinel powder has been obtained in two molar ratios of $MgO : Al_2O_3$ - 50:50 and 45:55.* These powders will be used in the pressure sintering studies and some of the specimens formed from them will later be utilized in the diffusion studies.

All pressure sintering runs will be made in the Vacuum Industries hot press located in Coxe Laboratory. The die assembly will consist of TZM punches and a die body having a graphite liner. Graphite spacers will be placed between the plungers and the powder so that the powder is surrounded by a graphite environment.

The ram displacement during the run will be monitored with an LVDT driving an X-Y plotter. By measuring the final height of the specimen the instantaneous strain rate at any point in the run can be calculated from the ram displacement versus time data after suitable corrections are made for thermal expansion of the pressure train.

Pressure sintering runs will be made at temperatures between 1200° and 1500°C at pressures between 200 and 20,000 psi. The densification rate will be determined for each of the runs and the pressure-temperature regime where the relationship $\dot{\epsilon} = k\sigma^l$ is obeyed will be outlined.** The strain rate data obtained from this region will be analyzed by use of

* The powders were purchased from Dr. Morgan of the Franklin Institute Research Laboratory.

** Rummel and Palmour (24) have shown that the densification kinetics of magnesia-rich spinel obeyed this relationship in the range 1260° to 1450°C and 500 to 3000 psi applied pressure.

an appropriate densification model. A value of the apparent diffusion coefficient as a function of temperature will be determined and the activation energy for diffusion will be calculated from an Arrhenius-type relation.

The final grain size of each specimen will be measured and the strain rate dependence on grain size will be determined. Several pressure sintering runs will also be devoted to a determination of the grain growth kinetics of the specimens so that if necessary it would be possible to correct the model for changes in grain size with time.

Some preliminary data has been obtained and is given in the Appendix.

B. Diffusion Experiments

The diffusion experiments are designed so that the data obtained will compliment that obtained from the densification studies. These experiments will yield a value for the interdiffusion coefficient as a function of temperature and will also provide information of the effects of grain size on the diffusion rate.

A molydenum wire wound tube furnace obtained from Lamont Scientific Company will be used to perform the diffusion experiments. The oxygen partial pressure within the furnace will be controlled by passing a metered flow of a CO-CO₂ mixture over the diffusion couples.

Preliminary diffusion anneals are to be made with a single crystal of 50:50* spinel and a single crystal of 25:75* spinel making up each

* These ratios denote the molar ratio of MgO : Al₂O₃ in the compound.

sandwich-type diffusion couple. These anneals will be carried out at temperatures between 1200° and 1700°C for times varying between 10 hours and 150 hours. The resultant composition gradient across the diffusion couple interface will be determined by an ARL electron beam microprobe. The data will be analyzed by both the Matano (25) and the Wagner (26) methods and the cationic interdiffusion coefficient as a function of temperature will be calculated. An activation energy for diffusion will be determined by use of an Arrhenius-type relationship.

This preliminary study will enable the investigator to obtain familiarity with specimen preparation procedures and techniques of data analysis. The best method by which to analyze the data (either the Matano or the Wagner method) will be determined during this phase of the investigation and the results obtained will be compared to those of Whitney (27) who did work in the same system.

The remainder of the diffusion experiments will be directed toward the determination of cationic interdiffusion coefficients and activation energies for diffusion in polycrystalline spinel as a function of grain size and temperature. Prior to preparation of the diffusion couples, pressure sintered specimens of both compositions will be annealed at temperatures high enough to cause grain growth to occur. The temperatures will be selected so that grain sizes varying by approximately two orders of magnitude are obtained (for example, from $1\mu\text{m}$ to $100\mu\text{m}$).

Specimens with a molar composition ratio of 50:50 will be used as one half of the couple while the 45:55 spinel will be used as the other

half. The grain sizes of these two bodies will be matched as closely as possible. Diffusion couples will be placed in the furnace and annealed at a temperature ranging from 1200° to 1500°C. From analysis of the composition gradient through the couple after the anneal by use of an electron beam microprobe the interdiffusion coefficient will be determined. The specific mathematical analysis to be used will be determined from the studies on single crystals mentioned earlier. A temperature-grain size matrix will be set up so that from data obtained on a series of diffusion couples having different grain sizes and having been annealed at different temperatures the effects of grain size on the interdiffusion coefficient as a function of temperature can be determined. The activation energy for diffusion can then be obtained from an Arrhenius relationship between the interdiffusion coefficient and temperature.

After preliminary data from the densification studies and from the diffusion experiments are obtained and analyzed a committee meeting will be called to discuss the results. The purpose of this meeting is to determine the area which should receive the most emphasis in subsequent experiments.

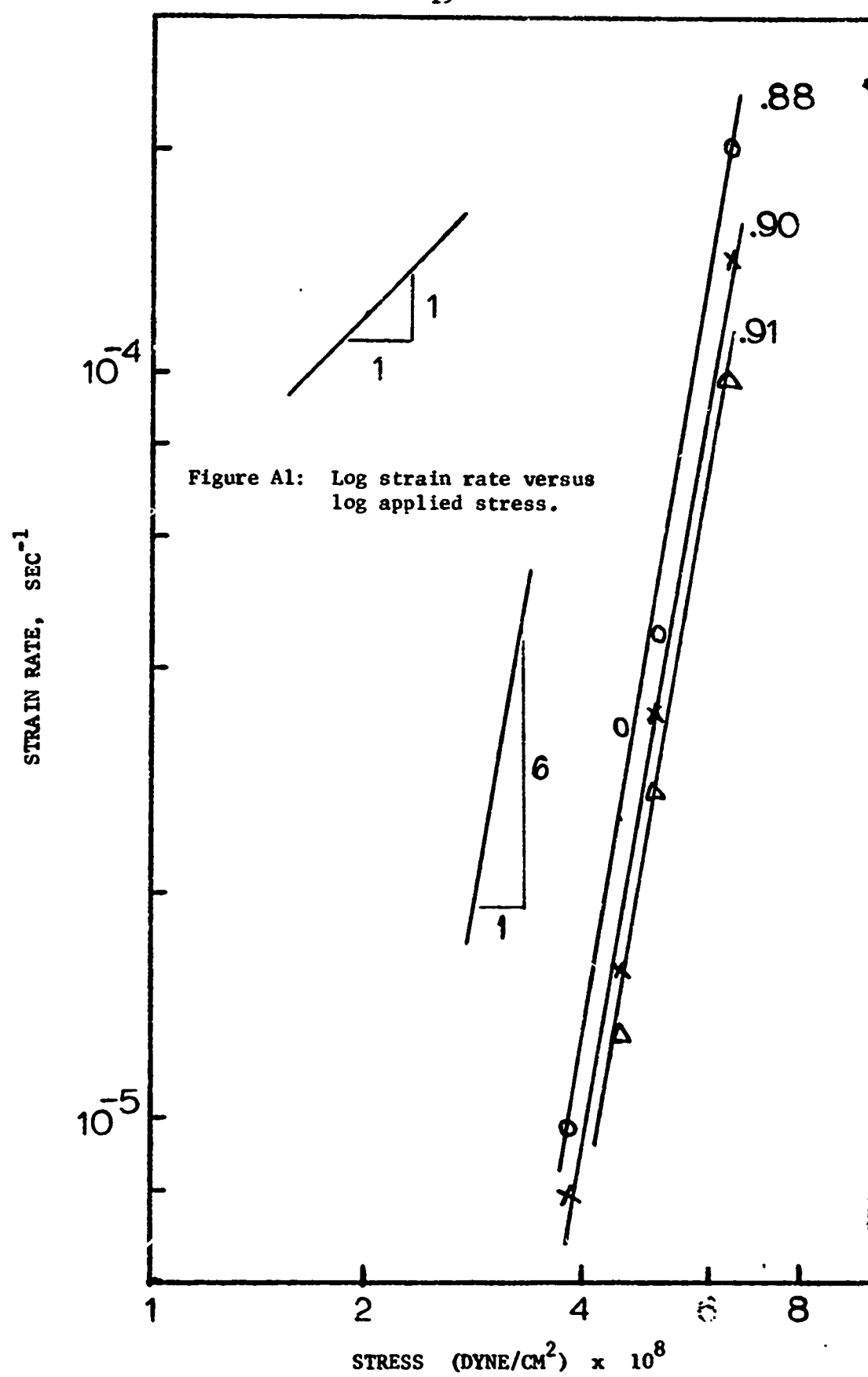
APPENDIX

Preliminary results have been obtained from pressure sintering studies on 45:55 ($\text{MgO} : \text{Al}_2\text{O}_3$ molar ratio) spinel at 1350°C and at applied pressures between 4000 and 9000 psi. An X-Y recorder with the Y-coordinate monitoring an LVDT attached to the hot press ram and the X-coordinate giving the elapsed time was used to record the data. The primary shrinkage data was taken from a dial gauge attached to the ram of the hot press and whose smallest division was 0.0001 inch.

The strain rate data obtained from the densification measurements was plotted as a function of applied stress at several porosity levels on a log-log scale. As seen in figure A1 the slope of the plots (equal to the stress exponent, n) was found to be equal to 6.

The high value for the stress exponent indicates a high strain rate sensitivity on stress. Values of n ranging from 4 to 6 have been theorized to indicate that a dislocation mechanism is operable during creep. However it has been shown that a change in creep mechanism occurs at lower stresses and that the value of n in this region of low stress is equal to 1 (28).

Because of this it has been decided that it is necessary to keep the applied stress below 5000 psi. In order to achieve final densities greater than 95% of theoretical densification studies will be carried out at temperatures between 1350° and 1500°C .



References

1. F. R. N. Nabarro, "Report of a Conference on the Strength of Solids", Physical Society, London, 1948, p. 75.
2. C. Herring, "Diffusional Viscosity of a Polycrystalline Solid", J. Appl. Phys. 21:437-45 (1950).
3. J. K. Tien and R. P. Gamble, "The Influence of Applied Stress and Stress Sense on Grain Boundary Precipitate Morphology in a Nickel-Base Superalloy During Creep", Met. Trans. 2:1663-1667 (1971).
4. R. C. Rossi and R. M. Fulrath, "Final Stage Densification in Vacuum Hot-Pressing of Alumina", J. Am. Ceram. Soc. 48:558-64 (1965).
5. J. D. McClelland, "A Plastic Flow Model of Hot Pressing", J. Am. Ceram. Soc. 44:526 (1961).
6. R. M. Spriggs and T. Vasilos, "Functional Relation Between Creep Rate and Porosity for Polycrystalline Ceramics", J. Am. Ceram. Soc. 47:47-48 (1964).
7. P. L. Farnsworth and R. L. Coble, "Deformation Behavior of Dense Polycrystalline SiC", J. Am. Ceram. Soc. 49:264-68 (1966).
8. R. L. Coble, "Diffusion Models for Hot Pressing with Surface Energy and Pressure Effects as Driving Forces", J. Appl. Phys. 41:4798-4807 (1970).
9. R. L. Coble, "A Model for Boundary Diffusion Controlled Creep in Polycrystalline Materials", J. Appl. Phys. 34:1679-1682 (1963).
10. R. C. Folweiler, "Creep Behavior of Pore-Free Polycrystalline Aluminum Oxide", J. Appl. Phys. 32:773-778 (1961).
11. S. I. Warshaw and F. H. Norton, "Deformation Behavior of Polycrystalline Aluminum Oxide", J. Am. Ceram. Soc. 45:479 (1962).
12. E. K. Beauchamp, et al., "Impurity Dependence of Creep of Al_2O_3 ", University of Utah, WADD Contract No. AF33(616)-6832, Project No. 0(7-7350) (1961).
13. R. Chang, "High Temperature Creep and Anelastic Phenomena in Polycrystalline Refractory Oxides", J. Nucl. Mater. 10:174-181 (1959).
14. B. Chandler, et al., "Fabrication and Properties of Extruded and Sintered BeO", J. Nucl. Mater. 8:329-347 (1963).

15. T. Vasilos and R. M. Spriggs, "Pressure Sintering of Ceramics", in Progress in Ceramic Science, Vol. 4, Pergamon Press, New York, 1966, pp. 95-132.
16. C. N. Alquist and R. A. Menezes, "Grain Boundary Sliding and the Observation of Superplasticity in Pure Metals", Mater. Sci. Eng. 7:223-224 (1971).
17. F. Garofalo, Fundamentals of Creep and Creep-Rupture in Metals, The Macmillan Co., New York, 1965, p. 128.
18. I. M. Lifshitz, "On the Theory of Diffusion-Viscous Flow of Poly-Crystalline Bodies", Soviet Physics, JETP 17:909-920 (1963).
19. R. Raj and M. F. Ashby, "On Grain Boundary Sliding and Diffusional Creep", Met. Trans. 2:1113-1127 (1971).
20. M. F. Ashby, "Boundary Defects and Atomistic Aspects of Boundary Sliding and Diffusional Creep", Contract N00014-67-A-0298-0020, NR-031-732, August, 1971.
21. R. C. Gifkins and K. U. Snowden, "Mechanism for Viscous Grain Boundary Sliding", Nature 212:916-917 (1966).
22. A. Miller, J. Appl. Phys. Supp. 30:24S (1959).
23. R. H. Arlett, "Interatomic Distances and Stability of Stoichiometric and Non-Stoichiometric Magnesium Aluminate Spinels: An Energetics Approach", Ph.D. Thesis, Rutgers University, 1967.
24. D. R. Rummel and H. Palmour, III, "Vacuum Hot-Pressing of Magnesium Aluminate Spinel", J. Am. Ceram. Soc. 51:320-326 (1968).
25. W. Jost, Diffusion in Solids, Liquids, Gases, Academic Press, Inc., New York, 1952.
26. C. Wagner, "The Evaluation of Data Obtained with Diffusion Couples of Binary Single-Phase and Multiphase Systems", Acta. Met. 17:99-107 (1969).
27. W. P. Whitney, II, "Interdiffusion Phenomena in the System MgO-Al₂O₃", Ph.D. Thesis, The Pennsylvania State University, 1970.
28. M. S. Seltzer, et al., "The Stress Dependence for High Temperature Creep of Polycrystalline Uranium Dioxide", J. Nucl. Mat. 34:351-353 (1970).

Appendix II

SURFACE FREE ENERGY AND WORK OF FRACTURE OF BRITTLE SOLIDS

D. P. H. Hasselman, J. A. Coppola and D. A. Krohn

Physical Ceramics Laboratory

Materials Research Center

Lehigh University

Bethlehem, Pennsylvania 18015

and

R. C. Bradt

Department of Materials Science

Ceramic Science Section

Pennsylvania State University

University Park, Pennsylvania 16802

ABSTRACT

A discussion is presented of the stress and energy criteria for brittle fracture. It is concluded that on thermodynamic grounds the stress criterion for catastrophic failure cannot be satisfied when the energy criterion for mechanical instability is met. It is suggested that the Griffith criterion defines the minimum stress level for crack propagation by a thermally activated process. Catastrophic crack propagation can be achieved by the expenditure of unrecoverable elastic strain energy in addition to the surface free energy of the new crack surfaces. It is estimated that the fracture surface energy of an entirely brittle material is at least three times the surface free energy. It is also concluded, contrary to widespread opinion, that surface free energy cannot be measured by means of a fracture experiment.

Introduction

The low tensile strength of brittle solids was attributed by Griffith to microcracks (1). In the formulation of his theory, Griffith hypothesizes that under conditions of thermodynamic reversibility, fracture will occur when on crack extension the change in energy of the stress field of the crack equals or exceeds the surface free energy of the resulting new fracture surfaces. This condition for crack instability can be expressed by:

$$\frac{dW}{dl} \geq 2\gamma_s \quad (1)$$

where W is the energy of the stress field of the crack, l is the crack length and γ_s is the surface free energy of the brittle material. Results of cleavage experiments on single crystals appear to establish the validity of this hypothesis (2-5).

Numerous recent studies, however, have shown that in many brittle solids even at low temperature the energy required to propagate a crack greatly exceeds the surface free energy, in apparent contradiction with the Griffith hypothesis. This discrepancy has been attributed to surface roughness and to energy dissipation processes such as plastic and viscous flow at the crack tip (6-13).

Without at this time wishing to present a complete review of brittle fracture, it is the purpose of this communication to suggest that the work required to propagate a crack in an entirely brittle solid indeed is expected to exceed the surface free energy. The excess energy consists of elastic strain energy which must be provided to bring the material to fracture but which cannot be recovered once fracture has taken place.

Discussion and Theory

Criteria of Fracture of a Brittle Fiber

The proposed concept of non-recoverable elastic energy, is illustrated most easily by considering the criteria for failure of a simple mechanical model, consisting of a uniaxially stressed fiber. The fiber is assumed to be entirely brittle and flaw-free and to exhibit linear elastic stress-strain behavior up to the interatomic cohesive fracture stress (σ_c). The load is applied at the fiber ends such that the stress is uniformly distributed along the total length of the fiber.

Mechanical stability of the fiber, under conditions of thermodynamic reversibility, which forms the basis for the Griffith theory, will be considered first. Under these conditions, at the critical stress the total potential energy in the fiber equals the total surface energy of the new fracture surfaces created on failure. For failure at a single planar cross section oriented perpendicularly to the fiber length, this condition occurs when:

$$\sigma_{cr}^2 L/2E = 2\gamma_s \quad (2a)$$

or

$$\sigma_{cr} = (4\gamma_s E/L)^{1/2} \quad (2b)$$

where σ_{cr} is the critical fracture stress under conditions of reversibility, L is the fiber length and E is Young's modulus of elasticity.

Failure of the fiber can also be considered from the point of view of the energy required to completely separate two adjacent atom planes at the interatomic cohesive stress (σ_c). Theories (14) for σ_c have shown that this requires a potential energy per interatomic distance of the order of $\sim \gamma_s$ per unit area of fracture plane. At the critical fracture stress, σ_{cr} of equation 2, it is easily calculated that the potential energy between two adjacent atom planes equals $2\gamma_s a/L$, where a is the interatomic distance. Since in any fracture experiment $L > a$, the energy density in the fiber at $\sigma = \sigma_{cr}$ is insufficient for fracture to occur. As a consequence over the stress range:

$$\sigma_{cr} < \sigma < \sigma_c \quad (3)$$

the fiber is mechanically unstable in a thermodynamic sense, but fracture will not take place since the stress condition for failure is not satisfied. It is still feasible, however, for fracture to occur over this stress range (equation 3) if the potential energy is redistributed to the plane of fracture by a thermally activated process. At low temperatures and long fiber length this appears unlikely.

By stressing any segment of the fiber to the cohesive fracture stress (σ_c), catastrophic failure can be achieved. However, in view of the loading conditions imposed, this requires stressing the fiber as a whole to this value of stress with an energy expenditure, i.e. the work of fracture (G) of the order:

$$G \approx 2\gamma_s (L/a) \quad (4)$$

On failure, the fraction of this energy in excess of the surface free energy of the new fracture surfaces is not recoverable as useful work, but is transformed into vibrational energy (i.e. heat, phonons, etc.) in the now stress-free fiber segments. It is absolutely essential, however, that this non-recoverable elastic strain energy be provided if fracture of the fiber of the fiber is to occur.

Criteria of Stability of a Crack in a Brittle Solid

Failure by the propagation of cracks in a brittle solid can be considered as the successive fracture of atomic bonds in the flaw-free material ahead of the crack tip. Energy and stress criteria such as those for the previously discussed fiber also apply to the stability and energy expended in the propagation of a crack. Plastic or viscous flow is assumed absent throughout the discussion.

In the Griffith theory the energy released on crack extension, dW/dl of equation 1, is obtained from the whole stress field surrounding the crack and not just from the crack tip alone. As a consequence, when the applied stress is such that equation 1 is satisfied, under conditions of thermodynamic reversibility, there is insufficient energy concentrated at the crack tip to provide the surface energy required for crack extension; catastrophic crack propagation simply cannot occur. On the basis, then, of energy consideration, at the condition of equation 1 the stress level at the crack tip cannot possibly be equal to the interatomic cohesive stress. This conclusion disagrees with Orowan's results (15) which suggest that the Griffith energy criterion also satisfies the critical stress condition for brittle fracture.

Crack propagation, however, can occur at the conditions of equation 1, if the energy of the stress field of the crack is transported to the crack tip by thermal means. This implies that the Griffith criterion, in fact defines the minimum stress condition required to cause crack growth by a thermally activated process rather than the stress condition for catastrophic fracture.

In analogy to the fiber, discussed above, the crack can be made to propagate in a catastrophic manner even at a very low temperature by raising the applied stress to a value such that the stress at the crack tip equals the interatomic cohesive stress. However, as for the previously discussed

fiber, the stress is applied at a site far removed from the tip of the crack. As a consequence, if the material at the crack tip is stressed to the cohesive stress, material adjacent to the plane of crack propagation must be stressed as well. This requires an expenditure of elastic strain energy in addition to the energy ($2\gamma_s$) required for creation of the new crack surfaces. It is the sum of these two energies that constitutes the work of fracture. As a result, the work of fracture measured in a fracture experiment constitutes the energy required to propagate a crack at a level of applied stress and a corresponding value of dW/dl (equation 1) such that the stress at the crack tip equals the interatomic cohesive stress. However, under these conditions fracture is not reversible and once crack propagation occurs, no mechanism exists by which the excess potential energy required for the initiation of crack propagation can be converted into useful work. It is merely dissipated into heat or vibration.

It is of interest to obtain an estimate for the work of fracture in terms of the energy and stress criteria as discussed above. For simplicity, due to the complex nature of the stress distribution near cracks, an estimate will be made of the total potential energy required to separate two neighboring atom planes at the interatomic cohesive stress with a stress field adjacent to the plane of fracture similar to the distribution of stress near the tip of a crack. As suggested by the Airy stress function (16), within a distance approximately one tenth of the crack size, the stress field near the crack tip can be expressed by:

$$\sigma = ky^{-\frac{1}{2}} \quad (5)$$

where k is a constant and y is the distance from a plane midway between the atom planes being separated. The constant k can be evaluated from the boundary condition: when $y = a/2$, $\sigma = \sigma_c$. This gives $k = \sigma_c (a/2)^{\frac{1}{2}}$ and:

$$\sigma = \sigma_c (a/2y)^{\frac{1}{2}} \quad (6)$$

Taking the stress distribution symmetric about $y = 0$ and noting that for $-a/2 < y < a/2$ the work done equals $2\gamma_s$, the total work in separating unit area of atom plane (i.e. the work of fracture) becomes:

$$G = 2\gamma_s + \int_{a/2}^R (\sigma_c^2 a/2yE) dy \quad (7)$$

where R represents the "range of influence", of the stress field at the tip of the crack. Setting $\sigma_c = (\gamma_s E/a)^{\frac{1}{2}}$ after (14), followed by integration yields:

$$G = 2\gamma_s + \frac{1}{2}\gamma_s \ln(2R/a) \quad (8)$$

To obtain a value for G that is more representative of the stress field of a crack, the multiaxial nature of the stress field can also be considered. Cook and Gordon (17) showed that, but for the immediate vicinity of the tip of a crack in a flat plate the stress is of a uniform biaxial nature. This introduces an additional factor $2(1-\nu)$ in the second terms of equation 8, where ν is Poisson's ratio, such that:

$$G = 2\gamma_s + (1-\nu)\gamma_s \ln(2R/a) \quad (9)$$

An estimate of G may be made on the basis of a numerical example. Conservatively estimating the range of influence, R , to extend over only one hundred interatomic distances (i.e. $R = 100a$), gives for $\nu = 0.25$:

$$G \approx 6.0\gamma_s \quad (10)$$

or, if preferred in terms of the fracture surface energy, $\gamma_f = G/2$:

$$\gamma_f \approx 3.0\gamma_s \quad (11)$$

This result suggests that in propagating a crack the additional energy required to stress material located within only one hundred interatomic distances already has the effect of nearly tripling the fracture surface energy. Since only one hundred interatomic distances were considered, equation 11 clearly represents an underestimate for γ_f . In addition, in polycrystalline materials surface roughness can easily lead to a further doubling or tripling of γ_f to a value perhaps as high as $10\gamma_s$. Regardless of the actual value, it is clear that the non-recoverable elastic strain energy can cause the fracture surface energy in an entirely brittle material to exceed the surface free energy by an appreciable amount. As a consequence, no need exists to resort to energy dissipation by plastic or viscous flow to completely explain the observed discrepancies between surface free energy and fracture surface energy. Clearly, energy dissipative processes such as plastic or viscous flow can contribute further to the work of fracture but they are not the sole mechanisms.

The present discussion leads to the inevitable conclusion that surface free energy of a brittle solid cannot be measured by means of a

fracture experiment using specimens of macroscopic size. Similar conclusions were also expressed by Bikerman (18) and Thompson et al. (19). Those studies in which fracture experiments result in apparent values of surface free energy need to be re-examined. Surface free energy in principle, can be measured by mechanical means by determining the minimum stress required for crack growth by a thermally activated process. At low temperature such experiments are expected to be time consuming.

The surface free energy (γ_s) is directly proportional to Young's modulus of elasticity as shown by Gilman (20). As a consequence from equation 11, which relates γ_f and γ_s , the fracture surface energy is also expected to be proportional to Young's modulus. Observations by Wiederhorn (10) on the fracture surface energy of various glasses with different values of Young's moduli are in support of this hypothesis.

An additional observation must also be made in relation to the interpretation of brittle fracture data. Since equation 1 represents the minimum energy condition required to render a crack thermodynamically unstable and equation 8 or 11 gives the energy required for catastrophic crack propagation, over the range:

$$2\gamma_s < dW/dl < G \quad (12)$$

the crack is unstable in a thermodynamic sense; catastrophic fracture will not occur but crack growth can take place by means of a thermally activated process. As a result, in any fracture experiment carried out at a temperature in excess of 0°K, some subcritical crack growth prior to catastrophic failure is to be expected.

The thoughts expressed in the present note can be used to qualitatively interpret the observations of Congleton, Petch and Shiels (21) for the temperature dependence of the fracture surface energy of polycrystalline aluminum oxide. At -196°C, these authors observed $\gamma_f \approx 3 \times 10^4$ ergs. cm^{-2} , decreasing to approximately 1.5×10^4 ergs. cm^{-2} at 250°C followed by a rapid increase to about 6×10^4 ergs. cm^{-2} at 500°C. Taking $\gamma_s \approx 2,000$ ergs. cm^{-2} and assuming that surface roughness is such that the actual surface area is doubled, equation 11 suggests a $\gamma_f \approx 1 \times 10^4$ ergs. cm^{-2} or even higher. As a result, at -196°C perhaps as much as one half of the value of γ_f can be attributed to non-recoverable elastic energy. The observed decrease in γ_f from -196°C to 250°C can be attributed to the

redistribution of elastic energy from the stress field of the crack to the crack tip. This reduces the applied stress required to raise the crack tip stress to the cohesive strength which manifests itself in an apparent decrease in the fracture surface energy. Only the increase in γ_f at temperatures above 250°C, in the opinion of the present writers, is due to plastic work as the result of increased dislocation mobility. Similar observations for the temperature dependence of the fracture surface energy have been reported by Coppola and Bradt for silicon carbide (22) and silicon nitride (23) and can possibly be explained by the above argument.

Summary

The present discussion points out that at the minimum energy requirement for mechanical instability under conditions of thermodynamic reversibility, stress requirements for catastrophic failure cannot be satisfied. Catastrophic fracture of an entirely brittle solid requires an expenditure of energy well in excess of the surface free energy, which is not recoverable on fracture.

Acknowledgments

The thoughts expressed in the present communication were the result of interaction between two research programs supported by the Pennsylvania Science and Engineering Foundation under contract ME-344-151 and by the U.S. Army Research Office - Durham, North Carolina, under grant DA-ARO-D-31-124-G1106, respectively.

References

1. A. A. Griffith, Proc. Roy. Soc. (London), 221A, 163 (1920).
2. J. J. Gilman, J. Appl. Phys., 31, 2208 (2208).
3. A. R. C. Westwood and D. L. Goldheim, J. Appl. Phys., 34, 3335 (1963).
4. P. L. Gutshall and G. E. Gross, J. Appl. Phys., 36, 2459 (1965).
5. Y. P. Gupta and A. T. Santhanam, Acta Met., 17, 419 (1969).
6. J. Nakayama, J. Am. Ceram. Soc., 48, 583 (1965).
7. F. J. P. Clarke, H. G. Tattersall and G. Tappin, Proc. Brit. Ceram. Soc., 6, 163 (1966).
8. R. W. Davidge and G. Tappin, J. Mat. Sci., 3, 165 (1968).
9. P. L. Gutshall and G. E. Gross, Engr. Fract. Mech., 1, 463 (1969).

10. S. M. Wiederhorn, J. Am. Ceram. Soc., 52, 99 (1969).
11. S. M. Wiederhorn, J. Am. Ceram. Soc., 52, 485 (1969).
12. A. G. Evans, Phil. Mag., 22, 84 (1970).
13. J. A. Coppola and R. C. Bradt, (submitted to J. Am. Ceram. Soc.).
14. A. S. Tetelman and A. J. McEvily, Jr., Fracture of Structural Materials, p. 45, John Wiley, New York (1967).
15. E. Orowan, Repts. Prog. Phys., XII, 185 (1948).
16. P. C. Paris and G. Sih, Special Technical Publication 381, p. 30, A.S.T.M., Philadelphia (1970).
17. J. Cook and J. E. Gordon, Proc. Roy. Soc. (London), 282, 508 (1964).
18. J. J. Bikerman, Phys. Stat. Sol, 10, 3 (1965).
19. R. Thompson, C. Hsieh and V. Rana, J. Appl. Phys., 42, 3154 (1971).
20. J. J. Gilman, Fracture, p. 193, M.I.T. Press, Cambridge (1959).
21. J. Congleton, N. J. Petch and J. A. Shiels, Phil. Mag., 19, 795 (1969).
22. J. A. Coppola and R. C. Bradt, Proc. Conf. on Mechanical Behavior of Materials, Kyoto, Japan (1971).
23. J. A. Coppola and R. C. Bradt, (to be published).

Appendix III

The Griffith Approach to Brittle
Fracture and Plastic Flow in Glass

by

David A. Krohn

Physical Ceramics Laboratory
Materials Research Center

and

Department of Metallurgy and Material Science
Lehigh University
Bethlehem, Pa. 18015

Abstract

The Griffith approach to brittle fracture is considered with the emphasis on fracture surface energy. The reversible concept of brittle fracture is modified to include the irreversible processes accompanying the creation of new fracture surfaces. These processes are reviewed with regard to their effect on the true surface fracture energy. A model for "Dislocation-like" behavior is proposed and independent experimental support of this proposal is discussed.

Introduction

Glass is an isotropic material with an amorphous structure. It breaks in a brittle way with little or no apparent plastic deformation taking place. Since glass is observed to fracture under a critical uniaxial tensile stress, the maximum tensile stress is the criterion for failure⁽¹⁾. The fracture is always observed to be initiated from the surface for glass free of inclusions. The surface control of the fracture of glass is not surprising since sources of internal weakness associated with grain boundaries are not present.

Theoretically, the fracture strength of glass should equal the cohesive strength for breaking bonds^(1,2) (i.e., $E/10$ where E is Young's modulus). This means that for most glasses, the theoretical fracture strength should be on the order of 750,000-1,500,000 psi. Several investigators^(3,4) have observed strengths of this magnitude. However, the observed strengths of most glasses are reported to be between 10,000 and 50,000 psi. Griffith^(1,3) proposes that the difference between theoretical strengths and those experimentally observed is due to the presence of small cracks which act as stress concentrators. When the material is stressed, the theoretical strength is reached in small volumes of glass even though the average stress is low.

Griffith Approach

Griffith⁽³⁾ proposes that the unstable propagation of a crack must result in a decrease in free energy of the system. The source of energy for crack propagation is the release of strain energy which goes into creating the new surface. The total free energy μ_t of the system containing a crack is of the form:

$$\mu_t = \mu - \mu_E + \mu_s \quad (1)$$

$$\mu = \frac{\sigma^2 V}{2E} \quad (2)$$

$$\mu_E = \frac{\pi \sigma^2 C^2}{E} \quad (3)$$

$$\mu_s = 4C\gamma s \quad (4)$$

where: μ = elastic strain energy when no cracks are present ($\mu \neq f(c)$)

μ_E = stored elastic strain energy which is released as the crack grows

μ_s = total surface energy resulting from the crack

σ = applied stress

C = $\frac{1}{2}$ crack length

γ_s = true surface free energy (work done in forming unit area of new surface as a result of breaking atomic bonds)

V = volume

The condition for crack growth is:

$$\frac{\partial}{\partial C} (\mu_s - \mu_E) \leq 0 \quad (5)$$

This equation indicates that a crack will grow when the incremental release of elastic strain energy is greater than the incremental increase of surface energy produced as the crack surfaces are generated. From equation 4 the Griffith equation is obtained

$$\sigma_{\text{fracture}} = \left(\frac{2E\gamma s}{\pi C} \right)^{\frac{1}{2}} \quad 34 \quad (6)$$

In a modified form, γ_s is replaced by γ , the fracture surface energy, (energy of formation of a unit area created by the fracture process⁽⁵⁾). The reason for this substitution will become evident in the following discussion.

Griffith^(3,5) considers that fracture is a reversible process. He indicates that the strains must be elastic and that cracks can be propagated or healed by increasing or decreasing the load. The energy absorbed during the surface formation is lost upon surface annihilation (healing). However, fracture is usually accompanied by irreversible processes such as plastic flow, viscous flow and irreversible chemical reactions. Wiederhorn⁽⁵⁾ indicates that these irreversible processes cause the fracture surface energy to be more or less than the true surface free energy. Plastic and viscous flow cause a shear displacement of material which prevents rehealing. Shear displacements increase the fracture surface energy because energy is expended during the deformation process. Stress corrosion prohibits rehealing by removing material and chemically altering the new surface. Stress corrosion decreases the fracture surface energy because the chemical reaction supplies energy for surface formation.

From the relation $\sigma(C)^{\frac{1}{2}} = \left(\frac{2Eys}{\pi}\right)^{\frac{1}{2}}$, Griffith⁽³⁾ using experimental values determined that the average value of $\sigma(C)^{\frac{1}{2}}$ was 239 psi (in)^{1/2} and $\left(\frac{2Eys}{\pi}\right)^{\frac{1}{2}}$ was 134 psi (in)^{1/2}. The discrepancy can be accounted for by considering that the true surface free

energy does not take irreversible processes into consideration. The value of γ_s used by Griffith was 0.003 lb/in. Wiederhorn⁽⁵⁾ measured the fracture surface energy of soda-lime-silica glass (similar to the glass that Griffith used) to be about 0.021 lb/in (3.82 joules/m^2) which reflects the irreversible processes. Griffith's value of surface energy (extrapolated to room temperature from high temperature surface tension data) is only about 15% of the measured value. In addition to not including irreversible processes, another possible large error is suggested by Morey^(5,6). At higher temperatures the structural elements of the glass are mobile and an equilibrium structure is present which has a minimum surface free energy. At lower temperatures, the glass components are not mobile and the nonequilibrium structure is characterized by a higher surface free energy than extrapolation would yield.

Plastic Deformation

Recently reported⁽⁷⁾ values of glass strength are highly reproducible and probably indicate a pristine surface condition. However, these values are still well below the theoretical cohesive strength. Also it has been observed that calculated fracture surface energies are as much as 50 times greater than the surface free energy⁽⁸⁾. Marsh⁽⁷⁾ indicates that an elastic-plastic theory could account for the discrepancies. This theory can be illustrated by considering that the random structure of glass causes it to be a non-work hardening solid. Glass has no stabilizing mechanism at the yield point and so must fail catastrophically when the applied stress equals the flow stress. The apparent complete brittleness of glass is a result of the fact that fracture occurs at the flow stress with negligible elongation. Marsh demonstrates plastic flow around indentations and scratch marks on glass specimens. He indicates that the plastic flow around indentations results from very high local stresses. Similar high stresses exist in the vicinity of crack tip just prior to failure and therefore plastic flow should occur.

Marsh⁽⁷⁾ proposes that the fracture criterion is that of a critical plastic zone size. Wiederhorn⁽³⁾ estimates the plastic zone size using Dugdale's model of plastic flow at the crack tip (see Figure 1).

The following assumptions are made in the model⁽³⁾: first the plastic zone extends a length R in front of the crack tip; second, the material within the plastic zone is at the yield stress of the solid. The plastic zone is given by⁽³⁾:

$$R = (\pi/8) (k_{lc}/\sigma_{ys})^2 \quad (7)$$

where k_{lc} is the critical stress intensity factor and σ_{ys} is the yield stress. The displacement at the crack tip is⁽³⁾:

$$V(c) = 4 \sigma_{ys} R / \pi E \quad (8)$$

Energy absorption is equal to $\sigma_{ys} V(c)$. Wiederhorn⁽⁵⁾ estimates the size of the plastic zone for soda-lime-silica glass to be 2.9×10^{-9} m and the crack opening displacement to be 4.5×10^{-10} m. He indicates that the dimensions are not much larger than the silicon-oxygen distance of 1.6×10^{-10} m or the oxygen-oxygen distance of 2.6×10^{-10} m. The very brittle nature of glass is a consequence of the small plastic zone size. Wiederhorn⁽⁵⁾ found that the energy absorption for a moving crack is about 4.5 joules/m² for soda-lime-silica glass as compared to about 10^4 joules/m² for metals for which the plastic zone is much larger than for glass. As a result for glass, as a crack begins to move it tends to propagate catastrophically. The energy absorption of 4.5 joules/m² is approximately equal to the measured surface fracture energy. Although this might seem conclusive for the plastic flow argument, Wiederhorn⁽³⁾ points out that the model uses a continuum mechanics approach and its validity is in question for such small plastic zone sizes.

In recent work, Wiederhorn⁽⁶⁾ shows that cracks in soda-lime-silica glass can heal. Cracks can heal only if proper alignment can be obtained when the crack faces are rejoined. The healing process is caused by atomic forces pulling the surfaces together. Distortions from plastic flow will keep the surfaces apart. Therefore, for cracks to heal, the crack tip displacement must be within the range of atomic forces in glass, i.e., less than 10×10^{-10} m. Considering the Dugdale model, the crack tip displacement is about 4.5×10^{-10} m which is within the range; therefore plastic deformation can occur and not prevent the healing process.

Several other theories have been proposed to explain the flow of glass around indenters and account for the high fracture surface energy. Viscous flow is a possible mechanism⁽¹⁰⁾. The strain field caused by the high stresses at the crack tip can cause a localized heating thus allowing the glass to flow viscously.

Lange⁽¹¹⁾ has recently calculated the degree of heating at the crack tip and found it to be about 200°C. This is well below the temperature region where viscous flow would be a reasonable factor.

Roughness⁽¹²⁾ of the surface must also be considered to explain the high fracture surface energy. If the fracture surface is rough, shows forking, or sub-surface cracks are formed, these will contribute to the fracture surface energy. The Griffith approach has a thermodynamic basis and irreversible losses to the surroundings owing to the second law of thermodynamics accompany the fracture process⁽¹³⁾.

Mackenzie^(14,15,16) suggests a qualitative model to explain the results of indentation hardness tests. The application of hydrostatic pressure to a glass results in an elastic compression and the recovery is complete when the load is removed. If while the glass is under compression, it is also subjected to a shear, interlocking of the network will result as indicated in Figure 2. This entanglement causes an apparent densification when the pressure is released.

The geometry of a pyramidal indentor gives rise to shear stresses when it is penetrating the sample. This suggests that densification by high pressure may be involved in the observed flow resulting from the indentation tests. MacKenzie⁽¹⁴⁾ indicates that partial recovery of the indentation volume flow is observed at temperatures much lower than the glass transition temperature (temperature where the glass can viscously relax). He indicates that the recovery is difficult to explain if it is assumed that the flow is caused by a viscous or a plastic flow mechanism. MacKenzie also observes that densification due to high pressure recovers at temperatures much below the glass transition. However, the fact that only partial recovery is observed indicates that perhaps plastic flow is also occurring.

Ernsberger⁽¹⁷⁾ using optical techniques has confirmed that densification does take place at the indentation. The experimental results do not rule out the possibility that densification and plastic flow can occur together. It should be pointed out that for plastic or viscous flow, the volume is conserved and for

densification the volume disappears. Taylor⁽¹⁸⁾ shows experimentally that the material displaced by the indentor which forms the raised lip is equal to the volume of the indentation. This conservation of volume supports a viscous or plastic flow mechanism. In view of the temperature limitations calculated by Lange, plastic flow is the more probable mechanism.

After consideration of all the proposed theories of flow, the experimental and theoretical evidence indicates that plastic flow is a possible energy absorbing mechanism in glass fracture.

Discussion of the mechanism of plastic flow is complicated by the absence of dislocations in glass. However, Levengood⁽¹⁹⁾ observes flaw patterns in glass which behave under the influence of stress and etching solutions in a manner similar to dislocations in crystals. He⁽²⁰⁾ also observes that etch pits in the glass under an applied stress act as a source for "dislocation-like" loops. From the dimensions of the source, he calculates a Burger's Vector. Levengood⁽²¹⁾ calculates that the energy to form a flaw is small and that they can easily be formed at stress levels much below that of fracture. By a plastic flow mechanism these flaws can combine to form a microcrack and lead to subsequent fracture. March⁽⁷⁾ and Ainsworth^(22,23) suggest a "dislocation-like" mechanism. Ainsworth shows that the flow of glass is related to the proportion of network modifiers in the structure. The addition of network modifiers introduces non-bridging oxygens which provide "loose ends" in the structure and allows flow by a mechanism analogous to half planes which terminate at dislocations

in crystals.

An attempt to expand on the dislocation-like mechanism is given in the following discussion. Figure 3 shows the Zachariasen type structure for silica glass. Also shown is the effect of adding a network modifier, in this case, sodium. The modifier breaks the continuous linking of oxygen tetrahedra and weakens the glass. For dislocation movement in a crystal, the extra half plane of atoms sits at an energy maximum. Forces to move the dislocation in one direction are balanced by forces in the other. Therefore, the force required to move the dislocation is small and plastic flow is readily observed⁽²⁵⁾. A similar argument can be applied to the modified glass structure pictured. The non-bridging oxygens have a negative charge while the sodium ions have a positive charge. As a rough approximation, the attractive forces exerted by Na^+ labeled 1 will be balanced by forces exerted by Na^+ labeled 2. However, unlike the crystal, in which the dislocations move by glide on a slip plane, to move the oxygen tetrahedra requires a great deal of force to distort the structure and several bonds must be broken. (For crystals, unit movement requires only that one bond be broken). The movement of non-bridging oxygens is one of tearing which follows no particular plane. The dislocation line is pictured in Figure 3 and will have a variable Burger Vector as discussed by Gilman⁽²⁶⁾. Since the flow stress is the stress at which numerous bonds are broken by a tearing mechanism, then it is also expected that this will be the fracture stress. This is in agreement with March's⁽⁷⁾ work. As an example, Marsh shows

the flow stress and the fracture stress for soda-lime-silica glass are 510,000 psi, and 520,000 psi respectively. From the above arguments, in the absence of modifiers in the structure, plastic flow would not occur. Then fused silica (with no modifiers) would be expected to fracture in a manner without plastic flow. This conclusion is consistant with Levingood's⁽²¹⁾ work in which he demonstrates that fused silica is more brittle than glasses containing modifiers. Schardin⁽²⁷⁾ has also demonstrated this point. He found that the ratio of the velocity of brittle cracks to the shear wave velocity decreased as network modifiers were added to the glass indicating a dissipative energy. For fused silica the ratio was the highest revealing the extreme brittleness.

Summary:

The Griffith approach to brittle fracture explains the difference between theoretical cohesive strength and observed fracture strength. Developments in the field of fracture mechanics have helped to understand the discrepancies between fracture surface energy and surface free energy. The original concept of fracture being a reversible process must be modified to include the irreversible processes which several investigators show to exist. For glass fracture, plastic flow should be considered and the thought that glass breaks in a completely brittle way is certainly in doubt. It seems unlikely that an entire technolcgy will develop around dislocation-like movement in amorphous solids as has happened for crystalline solids. However, it is interesting to speculate how flow can occur by dislocation-like mechanisms.

- (1) W. D. Kingery, Introduction to Ceramics, Wiley, New York, (1960) 603.
- (2) A. S. Tetelman and A. McEvily, Jr., Fracture of Structural Materials, Wiley, New York, (1967), 38-85.
- (3) A. A. Griffith, "Phenomena of Rupture and Flow in Solid" Phil. Trans. Roy. Soc. (London), A221, (4) (1920) 163-98.
- (4) S. Jurkov, Tech. Phys., USSR, 1, (4) (1935) 386.
- (5) S. M. Wiederhorn, "Fracture Surface Energy of Glass", J. Am. Cer. Soc., 52, (1969) 99-105.
- (6) G. W. Morey, Properties of Glass, 2nd Ed; Reinhold, New York, (1954), 91.
- (7) D. M. Marsh, "Plastic Flow and Fracture of Glass", Proc. Roy. Soc., A, 282 (1964) 33-43.
- (8) E. B. Shand, J. Am. Cer. Soc., 44, (1961) 21.
- (9) S. M. Wiederhorn and P. R. Townsend, "Crack Healing in Glass", 53, (9), (1970) 486-9.
- (10) W. B. Hillig, "Concerning the Creation and Stability of Pyramidal Hardness Impressions on Glass", Advances in Technology, Plenum Press, New York, (1958) 51-2.
- (11) F. F. Lange, "Non-Elastic Deformation During Fracture of Glass", Tech. Rept. 3, Office of Naval Research, Contract No. N00014-68-C-0323, NR 032,507 (1970).
- (12) J. W. Johnson and D. G. Holloway, "On the Shape and Size of the Fracture Zone on Glass Fracture Surface", Phil. Mag. 14 (130), (1966) 731-44.
- (13) G. R. Irwin, private communication.
- (14) S. Sakka and J. D. MacKenzie, "High Pressure Effects on Glass", J. Non-Crystalline Solids, 1, (1969) 107-42.
- (15) J. D. MacKenzie, High Pressure Effects on Oxide Glasses: I, Densification in Rigid State", J. Am. Cer. Soc. 46, (1963) 461.
- (16) J. E. Neely and J. D. MacKenzie, "Hardness and Low Temperature Deformation in Silica Glass", J. Material Sci., 3, (6), (1969), 603-9.

- (17) F. M. Ernsberger, "Strength Controlling Structures in Glass", Fracture, C. J. Osborn, ed., Butterworth, Washington, D. C. (1965) 120-40.
- (18) W. R. Taylor, "Plastic Deformation of Optical Glass", J. Soc. Glass Technol., 34, 157, (1950), 64-76T.
- (19) W. C. Levengood, "Experimental Method for Developing Minute Flaw Patterns in Glass", J. Appl. Phys. 30, (1959) 378-86.
- (20) W. C. Levengood, "Defect Mechanism in a Non Crystalline Solid", J. Appl. Phys. 32, (1961) 2525-33.
- (21) W. C. Levengood, "Bond Rupture Mechanisms in Vitreous Systems", Intern. J. Fracture Mech., 2, (2), (1966) 400-11.
- (22) L. Ainsworth, "The Diamond Pyramid Hardness of Glass in Relation to the Strength and Structure of Glass. Part I. An Investigation of the Diamond Pyramid Hardness Test Applied to Glass.", J. Soc. Glass Technol. 38, (1954) 479-500.
- (23) L. Ainsworth, "The Diamond Pyramid Hardness of Glass in Relation to the Strength and Structure of Glass. Part II. Silicate Glasses", J. Soc. Glass Technol. 38, (1954) 501-35.
- (24) B. E. Warren, "Summary of Work on Atomic Arrangements in Glass", J. Am. Ceram. Soc., 24, (1941) 256.
- (25) G. E. Dieter, Jr., Mechanical Metallurgy, McGraw-Hill, New York (1961) 97-8.
- (26) J. J. Gilman, "The Plastic Response of Solids", Dislocation Dynamics, Ed. A. R. Rosenfield, G. T. Hahn, A. L. Gement, R. T. Jaffee, McGraw-Hill, New York (1968) 61-7.
- (27) H. Schardin, "Velocity Effects in Fracture", Fracture, B. L. Auerbach, et al., eds., M.I.T. Press, Cambridge and Wiley, New York, (1959) 297-330.
- (28) W. H. Zachariasen, "Atomic Arrangements in Glass", J. Am. Chem. Soc. 54 [10] 3841-51 (1932).

- (17) F. M. Ernsberger, "Strength Controlling Structures in Glass", Fracture, C. J. Osborn, ed., Butterworth, Washington, D. C. (1965) 120-40.
- (18) W. R. Taylor, "Plastic Deformation of Optical Glass", J. Soc. Glass Technol., 34, 157, (1950), 64-76T.
- (19) W. C. Levengood, "Experimental Method for Developing Minute Fracture Patterns in Glass", J. Appl. Phys. 30, (1959) 378-86.
- (20) W. C. Levengood, "Defect Mechanism in a Non Crystalline Solid", J. Appl. Phys. 32, (1961) 2525-33.
- (21) W. C. Levengood, "Bond Rupture Mechanisms in Vitreous Systems", Intern. J. Fracture Mech., 2, (2), (1966) 400-11.
- (22) L. Ainsworth, "The Diamond Pyramid Hardness of Glass in Relation to the Strength and Structure of Glass. Part I. An Investigation of the Diamond Pyramid Hardness Test Applied to Glass.", J. Soc. Glass Technol. 38, (1954) 479-500.
- (23) L. Ainsworth, "The Diamond Pyramid Hardness of Glass in Relation to the Strength and Structure of Glass. Part II. Silicate Glasses", J. Soc. Glass Technol. 38, (1954) 501-35.
- (24) B. E. Warren, "Summary of Work on Atomic Arrangements in Glass", J. Am. Ceram. Soc., 24, (1941) 256.
- (25) G. E. Dieter, Jr., Mechanical Metallurgy, McGraw-Hill, New York (1961) 97-8.
- (26) J. J. Gilman, "The Plastic Response of Solids", Dislocation Dynamics, Ed. A. R. Rosenfield, G. T. Hahn, A. L. Gement, R. T. Jaffee, McGraw-Hill, New York (1968) 61-7.
- (27) H. Schardin, "Velocity Effects in Fracture", Fracture, B. L. Auerbach, et al., eds., M.I.T. Press, Cambridge and Wiley, New York, (1959) 297-330.
- (28) W. H. Zachariasen, "Atomic Arrangements in Glass", J. Am. Chem. Soc. 54 [10] 3841-51 (1932).

List of Captions

Figure 1. The Dugdale model of elastic-plastic deformation near a crack. (After Wiederhorn (9))

Figure 2. MacKenzie's model of network entanglement and apparent densification under the influence of an applied shear stress. (After MacKenzie⁽¹⁴⁾)

Figure 3. Zachariasen model for the structure of glass.
A. Fused Silica (After Zachariasen (28))
B. Soda-Silica Glass (After Warren (24))

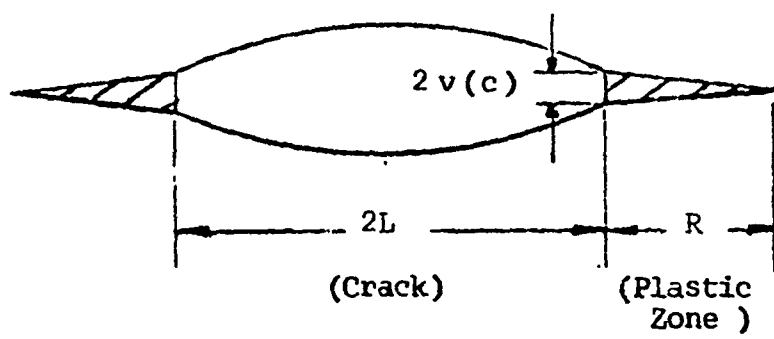
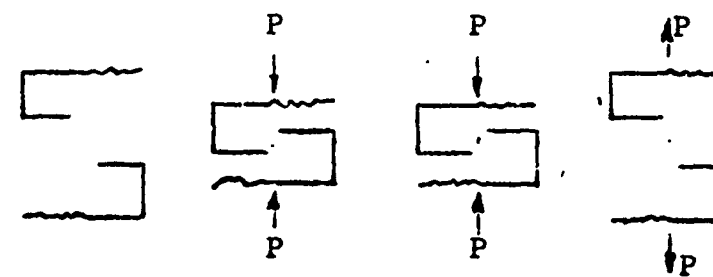
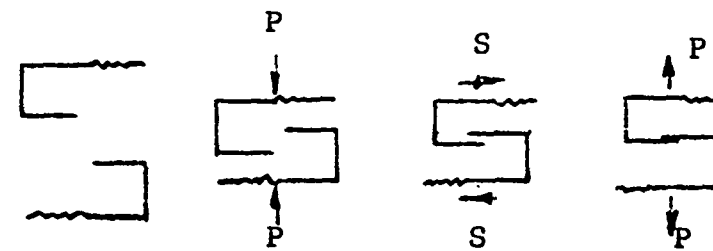


Figure 1

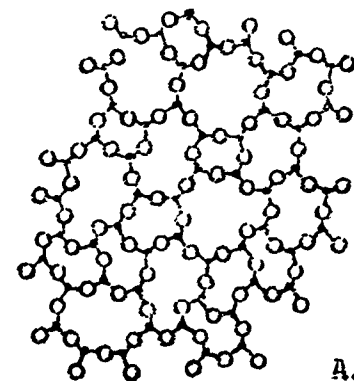


No Shear

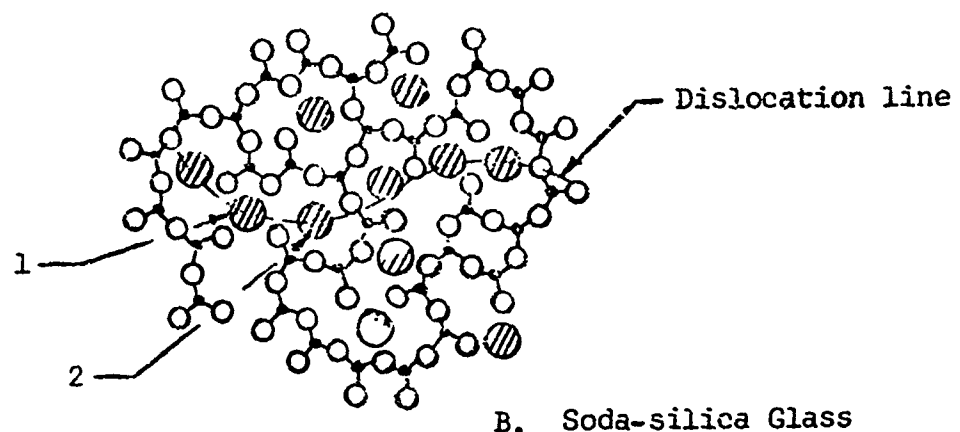


With Shear

Figure 2



A. Fused Silica



B. Soda-silica Glass

• = Si O = O \textcircled{N} = Na

Figure 3